Am J Cancer Res 2022;12(11):5226-5240
www.ajcr.us /ISSN:2156-6976/ajcr0146079

Original Article

KIF3A inhibits nasopharyngeal carcinoma proliferation, migration and invasion by interacting with β-catenin to suppress its nuclear accumulation

Zhe Hu[1], Jinlan Meng[2], Hongbing Cai[1], Na Ma[2], Xiujie Gao[2], Xiaojuan Li[1], Yan Xu[1]

[1]*Cancer Center, Integrated Hospital of Traditional Chinese Medicine, Southern Medical University, Guangzhou 510315, Guangdong, China;* [2]*Department of Physiology, School of Life Sciences and Biopharmaceutics, Guangdong Pharmaceutical University, Guangzhou 510006, Guangdong, China*

Received August 22, 2022; Accepted November 12, 2022; Epub November 15, 2022; Published November 30, 2022

Abstract: Nasopharyngeal carcinoma (NPC) is a malignant epithelial tumor prevalent in southern China and Southeast Asia. Previous studies have shown that Kinesin Family Member 3A (KIF3A) plays a critical role in the oncogenesis of various cancer types. However, the role of KIF3A in NPC tumorigenesis and the mechanism underlying its function have not been reported. In this study, we found that KIF3A was significantly downregulated in NPC cells and tissues, and KIF3A expression in NPC patients was associated with tumor stage and was positively corrected with overall survival. In vitro and in vivo experiments indicated that overexpression of KIF3A inhibited NPC cell proliferation, migration, and invasion. Mechanistic studies found that KIF3A bound β-catenin and attenuated β-catenin aggregation in the nucleus. Moreover, rescue experiments demonstrated that the inhibitory effect of KIF3A on NPC proliferation, migration and invasion was partially dependent on β-catenin. Taken together, our data suggest that KIF3A interacts with β-catenin and attenuates NPC proliferation, migration, and invasion by suppressing the intranuclear aggregation of β-catenin. KIF3A may be a promising therapeutic target of patients with NPC.

Keywords: Nasopharyngeal carcinoma, kinesin family member 3A, proliferation, migration

Introduction

NPC, a malignancy of epithelial cell origin in the head and neck, occurs frequently in Southern China and Southeast Asia and is closely related to Epstein-Barr virus infection, the environment, and the genetic factors [1-6]. There were 133354 new cases of NPC worldwide in 2020, accounting for 0.7% of all new cancer cases [7]. Although patients with early-stage NPC can be cured by radiation therapy alone, patients with advanced stage NPC have a poor 5-year survival rate due to recurrence and distant metastasis. Therefore, it is imperative to understand the molecular mechanisms underlying the progression of NPC and to identify novel diagnostic biomarkers.

KIF3A, a member of the kinesin protein family located on human chromosome 5q31.1, plays an essential role in intraflagellar transport (IFT) and assembly as well as mammalian cilia maintenance [8]. In addition, KIF3A is involved in a variety of cellular processes, including organelle and macromolecule transport, early development, cell migration, and tumorigenesis [9-11]. Consistently, loss of KIF3A decreases oligodendrogenesis and affects fine motor coordination [12]. Mechanistically, KIF3A and KIF3B dimerize and bind to RNF33, which in turn promotes kinesin-dependent cargo movement along the microtubules of the testes in mice [13]. In addition, KIF3A also helps heterodimeric KIF3AC convert microtubule trails to navigate intersections [14]. Notably, the life cycle of HIV in primary macrophages is regulated by KIF3A [15], and phosphorylation of KIF3A is crucial for US3-mediated immune escape during HSV-1 infection [16].

Furthermore, KIF3A has been reported to function as a tumor promoter and enhance the proliferation and metastasis of prostate cancer, triple-negative breast cancer, and bladder cancer [17-19]. Moreover, KIF3A is essential for medulloblastoma initiation and progression

[20]. Concurrent loss of both KIF3A and VHL promotes precursor lesions of clear cell renal cell carcinoma [21]. Silencing KIF3A in thyroid cancer cell lines leads to defective ciliogenesis, thereby promoting mitochondria-dependent apoptosis [22]. In contrast, KIF3A has been reported to interact with β-arrestin to function as a tumor suppressor in lung cancer via inhibiting the Wnt/β-catenin pathway [23]. A subsequent study also demonstrated the tumor suppressive role of KIF3A in lung cancer [24]. These studies indicate the complex role of KIF3A in different types of tumors; however, the biological role of KIF3A in NPC and its functional mechanism remain to be elucidated.

In this study, we first observed that downregulated expression of KIF3A was an unfavorable factor in the prognosis of NPC. Further experiments indicated that KIF3A suppressed NPC growth, migration, and invasion by interacting with β-catenin to inhibit Wnt/β-catenin pathway and the downstream epithelial-mesenchymal transition (EMT) related markers N-cadherin and vimentin as well as cell cycle regulators. Our results suggest that KIF3A might function as a tumor suppressor in NPC.

Materials and methods

Tissue specimens

A total of 106 paraffin-embedded NPC and 22 noncancerous nasopharyngeal epithelial specimens were collected from Nan Fang Hospital of Southern Medical University. Written consent form was obtained from patients. This study was approved by the Ethics Committee of TCM-Integrated Hospital of Southern Medical University.

Cell culture

The NPC cell lines HONE1, SUNE1, NP69 and 5-8F were obtained from the Cancer Research Institute of Southern Medical University (Guangzhou, China). These cells were cultured in RPMI 1640 (Biological Industries) supplemented with 10% foetal calf serum (Cegrogen, Germany) and maintained in a humidified chamber with 5% CO_2 at 37°C.

Immunohistochemistry (IHC) and survival analysis

The expression levels of KIF3A were examined by IHC, and the streptavidin-peroxidase conjugated method was used to visualize the staining signals according to the manufacturer's instruction (ZSGB-BIO). The staining results were independently evaluated by two pathologists. Staining intensity was scored by 0 to 3: 0 (negative staining), 1 (weak staining), 2 (moderate staining) and 3 (strong staining). Percentage staining was evaluated on a scale of 0 to 4: 0 (no staining), 1 (less than 25%), 2 (26-50%), 3 (51-75%), and 4 (76-100%). The intensity score multiplied by the percentage score was used as the immunohistochemical score. An immunohistochemical score > 6 was considered high expression, while a score ≤ 6 was considered low expression. The antibody used in IHC was anti-KIF3A (Proteintech, 1:100). Kaplan-Meier analysis was performed to plot survival curves, and the log-rank test was utilized to calculate *p* values.

Reverse transcription-quantitative PCR (RT-qPCR)

Total RNA from NPC cells was isolated using Cell Total RNA Isolation Kit (Foregene, China) according to the manufacturer's instruction. The RNA concentration was measured by Multiskan Sky Full-wavelength Enzyme Labeler (ThermoFisher Inc), and cDNA was generated with a reverse transcription kit (TaKaRa Company) in a Bio-Rad T100 Thermal Cycler. Subsequently, the cDNA was used as template and amplified with specific primers in a Roche Light Cycler. SYBR-Green (ACCURATE BIOLOGY) was used for qPCR detection. The PCR cycling conditions were as follows: 10 sec at 95°C, followed by 45 cycles for 10 sec at 95°C, 1 min at 60°C and 1 sec at 72°C, and 1 cycle of cooling for 30 sec at 50°C. The fold changes in KIF3A gene expression were analyzed by the $2^{-\Delta\Delta Ct}$ method. The primer sequences were as follows:

KIF3A forward: 5'-TCCCGTTCCCATGCCATCTT-3', KIF3A reverse 5'-GCTTCCTTTAGGCGCTGTCC-3', β-actin forward: 5'-ACAGAGCCTCGCCTTTGCC-3', β-actin reverse: 5'-GATATCATCATCCATGGTGAGCTGG-3'.

In vivo tumorigenesis in nude mice

All in vivo studies were performed following the protocol approved by the Ethics Committee of the TCM-Integrated Hospital of Southern Medical University. The human KIF3A gene was cloned into a lentivirus vector (LV-KIF3A) (GeneChem, Shanghai, China) which was used

to generate KIF3A-expressing SUNE1 cells. The empty lentivirus vector (LV-NC) was used as a control. Approximately 4 × 10^6 LV-NC or LV-KIF3A SUNE1 cells in the logarithmic phase of growth were subcutaneously injected into the flank of 4-week-old female nude mice (BALB/c, nu/nu) (n=7). After 15 days, the nude mice were sacrificed, and the tumor tissues were removed and weighed.

Western blot analysis

Briefly, NPC cells were lysed using RIPA Lysis buffer (Strong, CWBIO), and total protein concentration was quantified by BCA protein assay kit (TIANGEN Inc). Next, the proteins were separated by 10% or 12.5% SDS-PAGE and subsequently transferred onto a PVDF membrane. After blocking with 5% skim milk for 1.5 hours at room temperature, the membranes were incubated with the following primary antibodies: anti-KIF3A (Proteintech, 1:1000), anti-β-catenin (Proteintech, 1:2000), anti-N-cadherin (Proteintech, 1:1000), anti-vimentin (Proteintech, 1:1500), anti-c-Myc (Proteintech, 1:1000), anti-CCND1 (Proteintech, 1:1000), GAPDH (Bioworlde, 1:5000), and β-actin (Bioworlde, 1:5000) at 4°C overnight, followed by incubation with secondary horseradish peroxidase (HRP)-conjugated antibodies. GAPDH and β-actin were used as the loading control for normalization. Antibody binding signals were detected by a chemiluminescence imaging system (Minichemi™).

Small interfering RNA (siRNA), plasmids, and cell transfection

siRNA targeting KIF3A (siKIF3A) and scramble siRNA negative control (siNC) were synthesized by RiboBio (Guangzhou, China). The three siRNA sequences targeting KIF3A were as follows: siKIF3A-1: 5'-CTGCGTCAGTCTTTGATGA-3'; siKIF3A-2: 5'-CTTCGACTTCAGATGCTTA-3'; siKIF3A-3: 5'-AGGCTAGAGCTGAATTAGA-3'. The Wnt pathway specific inhibitor pyrvinium pamoate was purchased from MedChemExpress. The final concentration of siRNA/pyrvinium pamoate used in our experiments was 100 nmol/l. KIF3A and β-catenin overexpression plasmids were purchased from WZ Biosciences Inc (Shandong, China). For cell transfection, 8-12 h before transfection, HONE1 and SUNE1 cells were plated in six-well plates at 50-60% confluence, and plasmids or siRNAs were transfected into cells by using Lipofectamine TM 3000 (Invitrogen) according to the manufacturer's protocol. After 24-72 h culture, the cells were harvested for further analysis.

Cell Counting Kit-8 (CCK-8) and 5-ethynyl-2'-deoxyuridine (EdU) incorporation assays

Cell proliferation was measured by CCK-8 assay (Vazyme). Briefly, NPC cells were seeded into 96-well plates at 1500 cells/100 μl per well and cultured overnight. Before measurement, 10 μl of CCK-8 reagent was added to the wells for 1.5 h, and the optical density (OD) at 450 nm was measured using Multiskan Sky Full-wavelength Enzyme Labeler (ThermoFisher Inc). Cell viability was measured from Day 1 to Day 4.

EdU incorporation assay was conducted with a Cell-Light EdU Apollo 567 kit (RiboBio). Briefly, NPC cells were seeded into 96-well plates, and EdU A solution was added to the wells for 2 h. Cells were then fixed with 4% paraformaldehyde, permeabilized with 0.2% Triton X-100, followed by incubation with apollo solution for 30 min for cell nuclei staining. DAPI was added to stain the cell nuclei for 10 min. The cells were imaged under inverted fluorescence microscope (Olympus Corporation).

Colony formation assay and cell cycle analysis

For colony formation assay, NPC cells (100/well) were seeded into six-well plates and cultured for 2 weeks. The culture medium was renewed every 72 h. The cells were then fixed with 4% paraformaldehyde for 10 min and stained with crystal violet. Cell cycle analysis was performed according to the instructions of the Cell Cycle and Apoptosis Kit (Leagene).

Migration and Invasion assays

Transwell chamber was used to measure the migration and invasion capability of NPC cells. Briefly, 1 × 10^5 cells in serum-free RPMI 1640 were added to the upper chamber of Transwell plates. The upper side of chamber membrane was coated with (for invasion assay) or without BD Matrigel (for migration assay) (Corning). Complete RPMI 1640 supplemented with 10% foetal bovine serum (Cegrogen, Germany) was added to the lower chamber of the Transwell plates. After culture for 12-20-h, the cells mig-

rated or invaded to the bottom side of membrane were fixed with paraformaldehyde and stained with Giemsa (Nanjing JianCheng Technology) for 5 min. The cells were then counted and photographed under microscope.

Wound healing assay

For the wound healing assay, NPC cells were grown to approximately 90% confluence in 6-well plates, and a 100 ul pipette tip was used for wound scratching. The NPC cells were then cultured in serum-free medium, and the reduction of the wound area was imaged under an inverted microscope (Olympus Corporation) at 0 and 24/36 h.

Coimmunoprecipitation (Co-IP)

Briefly, total NPC cell lysates were subjected to immunoprecipitation with anti-IgG, anti-β-catenin, or anti-KIF3A antibodies overnight at 4°C. Then, protein A/G Magnetic beads (Bimake) were added to the lysates for 30 min at 37°C to precipitate the antigen-antibody complexes. After washing the beads twice with washing buffer, the precipitated complex was eluted, separated by SDS PAGE, and detected by western blot.

Immunofluorescence

NPC cells were seeded in 35-mm glass bottom cell culture dishes (SORFA LIFE SCIENCE, Zhejiang) and cultured overnight. The cells were then fixed with 4% paraformaldehyde, permeabilized with 0.2% Triton X-100, and incubated with the indicated antibodies overnight at 4°C. The cells were then incubated with fluorescent-labelled secondary antibodies at 37°C for 60 min, and DAPI was used to stain the cell nuclei. The cells were photographed under a confocal microscope.

Nuclear and cytoplasmic fractionation

Nuclear and cytoplasmic fractions were obtained using NE-PER Nuclear and Cytoplasmic Extraction reagents (Thermo Scientific) according to the manufacturer's instructions. Briefly, NPC cell pellets were lysed with ice-cold cytoplasmic extraction reagent (CER) I for 10 min at 4°C. Next, ice-cold CER II was added to the lysates for 1 min at 4°C, and the supernatants (cytoplasmic extracts) were obtained by centrifugation at 16,000 × g for 5 min. The remaining pellets were washed with wash buffer and resuspended in ice-cold nuclear extraction reagent (NER) for 40 min at 4°C. Finally, the lysates were centrifuged at 16,000 × g for 15 min, and the supernatants were saved as nuclear extracts.

Statistical analysis

GraphPad Prism 9 software was used for statistical analysis. The data were expressed as the mean ± SD from at least three independent experiments. Student's t test was performed to compare two groups, and comparisons among multiple groups were conducted using one-way analysis of variance (ANOVA). A p value of less than 0.05 was considered statistically significant.

Results

Decreased KIF3A expression correlated with the clinicopathological characteristics and the prognosis of NPC patients

To explore the role of KIF3A in NPC development, we first analyzed the expression of KIF3A in NPC samples using GSE64634 dataset. As shown in **Figure 1A**, KIF3A mRNA level was significantly downregulated in NPC tissues compared to control normal tissues. We then validated this finding experimentally in NPC cell lines by RT-qPCR and western blot. Consistently, KIF3A expression was notably downregulated in NPC cells compared with NP69 cells (nonmalignant nasopharyngeal epithelial cells) (**Figure 1B**, **1C**). Furthermore, we examined KIF3A expression in 106 NPC tissues and 22 noncancerous nasopharyngeal epithelial tissues by IHC and found that the expression of KIF3A was significantly reduced in NPC tissues compared with noncancerous nasopharyngeal epithelial tissues (p=0.018) (**Table 1**) (**Figure 1D**). Moreover, when comparing the clinicopathological characteristics of the NPC patients (**Table 2**), we found that decreased KIF3A expression was positively correlated with T stage (T1-T2 vs. T3-T4, p=0.035) and M stage (M0 vs. M1, p=0.039) but did not correlate with other clinicopathological characteristics. In support with this, survival analysis indicated that NPC patients with low KIF3A expression (n=63) had shorter survival times than patients

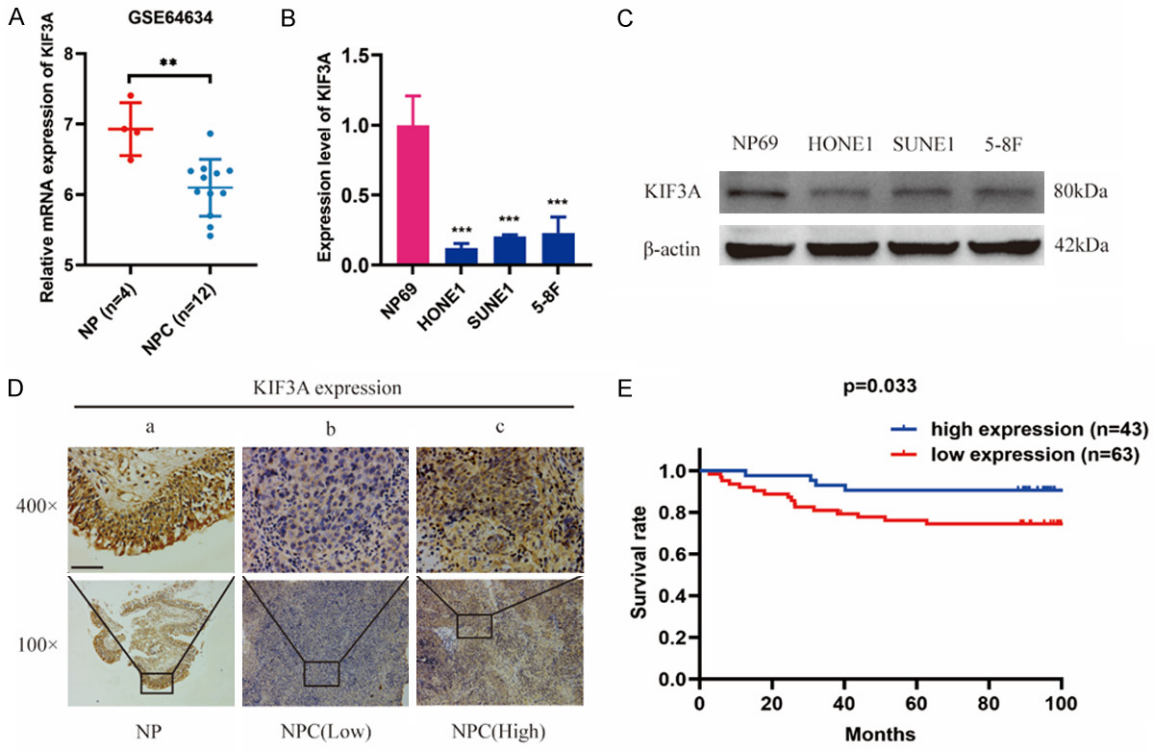

Figure 1. Decreased KIF3A expression correlates with the clinicopathological characteristics and prognosis of NPC patients. A. The relative mRNA expression of KIF3A in NPC tissues and normal tissues. B, C. RT-qPCR and western blot were performed to determine the mRNA and protein levels of KIF3A in NP69, HONE1, SUNE1, and 5-8F cells. D. KIF3A expression in nasopharyngeal epithelium and NPC samples by IHC. Typical immunohistochemical images were shown (Scale bar: 40 μm). a: Strong staining of KIF3A in NP tissues; b: low expression of KIF3A in NPC tissues; and c: high expression of KIF3A in NPC tissues. E. Kaplan-Meier survival analysis of the survival rates of NPC patients based on KIF3A expression. The log-rank test was used to calculate *p* values. *P < 0.05, **P < 0.01, ***P < 0.001.

Table 1. The expression of KIF3A in NPC and Normal epithelium

Group	Cases (n)	KIF3A expression		χ^2 value	*P* value
		Low	High		
NPC	106	63 (59.4%)	43 (40.6%)	5.607	0.018
Normal epithelium	22	7 (31.8%)	15 (68.2%)		

χ^2 test was used to access the expression of KIF3A in NPC and normal Nasopharyngeal epithelium tissues. NPC: Nasopharyngeal Carcinoma.

with high KIF3A expression (n=43) (log-rank test, p=0.033, **Figure 1E**).

KIF3A suppressed NPC proliferation in vitro and in vivo

To determine the effect of KIF3A on cell growth, we overexpressed KIF3A in HONE1 and SUNE1 cells by cell transfection. The overexpression efficiency of KIF3A was confirmed by western blot (**Figure 2A**). Then, CCK-8 and colony formation assays were conducted to compare the growth between vector-expressing and KIF3A-overexpressing cells. As shown in **Figure 2B**, **2C**, the growth of KIF3A-overexpressing/LV-KIF3A NPC cells was markedly attenuated compared with that of the NC/LV-NC cells. Furthermore, EdU incorporation assays and cell cycle analysis showed that the cell cycle progression of KIF3A-overexpressing cells was significantly inhibited compared with that of NC cells (**Figure 2D**, **2E**). To further demonstrate the role of KIF3A in tumor growth in vivo, we used xenograft tumor model by subcutaneously injecting LV-NC or LV-KIF3A SUNE1 cells into nude mice. After 15 days, the mice inoculated with LV-KIF3A SUNE1 cells exhibited lower tumor weights than the mice inoculated with LV-NC SUNE1 cells (**Figure 2F**). Taken together, these results demonstrated that KIF3A overexpression suppressed the growth of NPC cells both in vivo and in vitro.

Table 2. The relationship between the clinicopathologic characteristics and KIF3A expression in NPC

Factors		n	KIF3A expression		χ^2	*P* value
			Low	High		
Age (y)	< 50	52	34	18	1.499	0.221
	≥ 50	54	29	25		
Gender	Male	73	45	28	0.475	0.491
	Female	33	18	15		
Clinical stage	I-II	34	23	11	1.4	0.237
	III-IV	72	40	32		
T stage	T1-T2	51	25	26	4.422	0.035
	T3-T4	55	38	17		
N stage	N0-N1	62	37	25	0.004	0.952
	N2-N3	44	26	18		
M stage	M0	96	54	42	4.279	0.039
	M1	10	9	1		

NPC: Nasopharyngeal Carcinoma.

KIF3A suppressed NPC cell migration and invasion in vitro

To investigate the influence of KIF3A on NPC cell migration and invasion, we first performed wound healing assay and observed that KIF3A-overexpressing HONE1 and SUNE1 cells had significantly suppressed wound closure ability compared with NC HONE1 and SUNE1 cells (**Figure 3A**, **3B**). Next, Transwell assays showed that the overexpression of KIF3A significantly inhibited the migration and invasion of HONE1 and SUNE1 cells (**Figure 3C**, **3D**). Furthermore, we analyzed the expression of cell cycle-associated proteins and the EMT-related markers N-cadherin and vimentin by western blot. We observed that the expression of CCND1, c-Myc, N-cadherin and vimentin was downregulated in KIF3A-overexpressing HONE1 cells and SUNE1 cells compared with those in NC cells (**Figure 3E**).

Knockdown of KIF3A promoted NPC cell proliferation

To support the conclusions from overexpression experiments, we used siRNA knockdown approach to study the effect of KIF3A on NPC cell growth. The efficient knockdown of KIF3A was determined by RT-qPCR and western blot, as KIF3A mRNA and protein levels in the siKIF3A-2/siKIF3A-3 group were significantly reduced compared with that in the siNC group in both HONE1 and SUNE1 cells (**Figure 4A**, **4B**). Then, CCK-8 and EdU incorporation assays were conducted, and the results indicated that the growth of the siKIF3A-2 and siKIF3A-3 expressing NPC cells was significantly enhanced compared to the growth of siNC expressing cells (**Figure 4C**, **4D**).

Knockdown of KIF3A promoted NPC cell migration and invasion

Similarly, we used siRNA knockdown approach to determine the effect of KIF3A knockdown on NPC cell motility. Wound healing assay showed that knockdown of KIF3A enhanced the wound closure ability of HONE1 and SUNE1 cells (**Figure 5A**, **5B**). In addition, Transwell assays indicated that the knockdown of KIF3A significantly increased the migration and invasion of HONE1 and SUNE1 cells (**Figure 5C**, **5D**). Consistently, knockdown of KIF3A significantly increased the expression c-Myc, CCND1, the EMT-related markers N-cadherin and vimentin in both HONE1 and SUNE1 cells (**Figure 5E**).

KIF3A interacted with β-catenin and suppressed β-catenin nuclear translocation

To explore the molecular mechanisms by which KIF3A represses NPC proliferation, migration, and invasion, we used the BioGRID database to predict potential proteins that interact with KIF3A. Interestingly, we found that β-catenin is a candidate KIF3A-interacting protein. In support with this, a previous study has reported that KIF3A interacts with β-catenin during spermatogenesis in *Eriocheir sinensis*; however, this interaction has not been reported in *Homo sapiens*. Therefore, we investigated whether there is an interaction and regulation between KIF3A and β-catenin.

First, we found that overexpression of KIF3A inhibited, while knockdown of KIF3A enhanced, β-catenin protein level (**Figure 6A**). Next, we performed a Co-IP experiment and revealed an interaction between KIF3A and β-catenin (**Figure 6B**). Furthermore, immunofluorescence demonstrated the colocalization of KIF3A and β-catenin in NPC cells (**Figure 6C**). Moreover, we used the nuclear and cytoplasmic fractions to analyze the distribution of β-catenin in the nucleus and cytoplasm and determined that

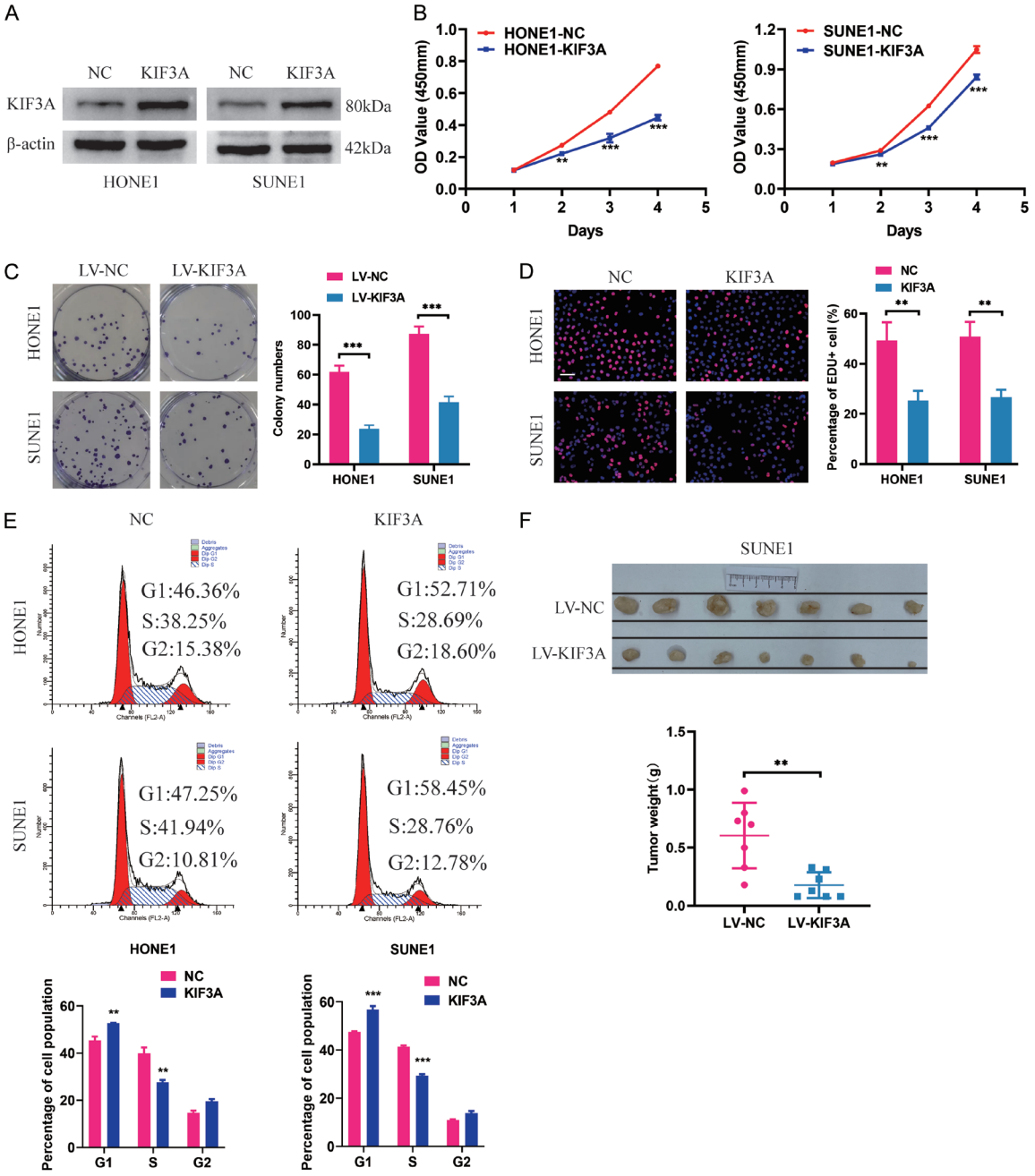

Figure 2. KIF3A suppresses NPC cell proliferation in vitro and in vivo. (A) KIF3A levels in vector- or KIF3A-expressing HONE1 and SUNE1 cells, as determined by western blot. (B) CCK-8 assay, (C) colony formation assay, (D) EdU incorporation assay (Scale bar: 100 μm) and (E) flow cytometry analysis were performed to evaluate the proliferation and cell cycle progression of vector- or KIF3A-expressing cells. Results were presented as the mean ± SD, Student's t test, **P < 0.01, ***P < 0.001. (F) The effect of KIF3A on tumor growth in vivo. A xenograft mouse model was generated by inoculating LV-NC or LV-KIF3A SUNE1 cells subcutaneously. Each group included 7 mice. Results were presented as the mean ± SD, Student's t test, **P < 0.01.

KIF3A overexpression suppressed β-catenin level in the cytoplasm and nucleus (**Figure 6D**). Together, these data demonstrated that KIF3A interacted with β-catenin in NPC and suppressed β-catenin nuclear translocation.

β-catenin reversed the inhibitory effect exerted by KIF3A overexpression in NPC

To further elucidate the role of β-catenin in KIF3A-regulated NPC phenotypes, we overex-

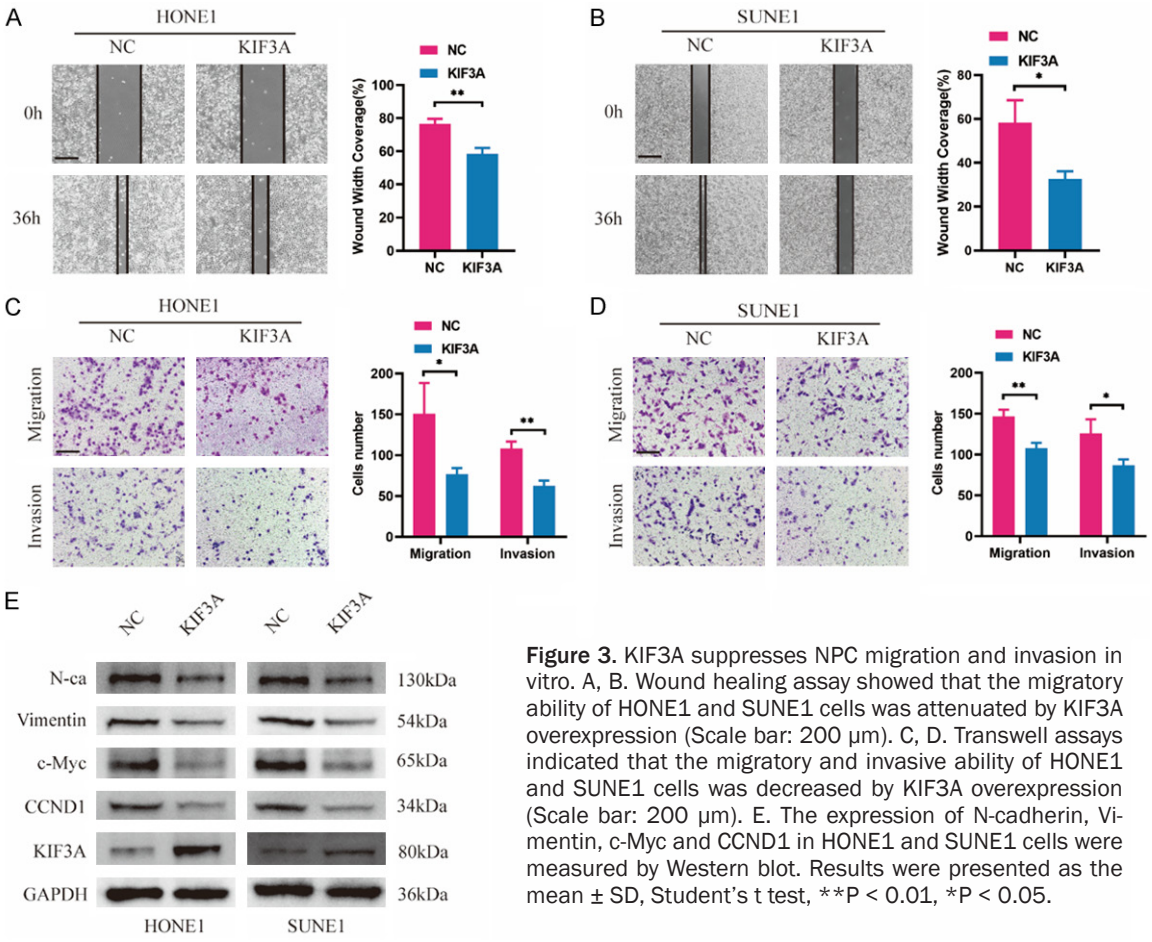

Figure 3. KIF3A suppresses NPC migration and invasion in vitro. A, B. Wound healing assay showed that the migratory ability of HONE1 and SUNE1 cells was attenuated by KIF3A overexpression (Scale bar: 200 μm). C, D. Transwell assays indicated that the migratory and invasive ability of HONE1 and SUNE1 cells was decreased by KIF3A overexpression (Scale bar: 200 μm). E. The expression of N-cadherin, Vimentin, c-Myc and CCND1 in HONE1 and SUNE1 cells were measured by Western blot. Results were presented as the mean ± SD, Student's t test, $^{**}P < 0.01$, $^{*}P < 0.05$.

pressed β-catenin in KIF3A stably overexpressing cells. EdU and Transwell assays showed that β-catenin overexpression reversed the inhibitory effects caused by KIF3A overexpression on cell proliferation and migration (**Figure 7A-D**). In addition, β-catenin overexpression attenuated the inhibitory effects of KIF3A overexpression on CCND1, c-Myc, N-cadherin, and vimentin protein levels (**Figure 7E**). Finally, pyrvinium pamoate, a specific inhibitor of the Wnt pathway, was used to treat KIF3A knockdown cells, and we observed that blocking Wnt pathway could reverse the effects induced by KIF3A siRNA (**Figure 7F**). Therefore, we concluded that β-catenin mediated the inhibitory effect exerted by KIF3A in NPC.

Discussion

Previous studies have shown the dual role of KIF3A in different cancer types, but the function of KIF3A and the underlying molecular mechanism in NPC have not been reported. Here, we first experimentally showed that KIF3A expression was downregulated in NPC cell lines and tissues compared to normal nasopharyngeal epithelial cells and tissues. Furthermore, survival analysis indicated that decreased KIF3A expression was associated with a worse prognosis for NPC patients, suggesting a tumor-suppressive role of KIF3A in NPC. These data were similar to the observation in lung cancer but were contrary to the observations in prostate cancer, triple-negative breast cancer, and bladder cancer [17-19, 23].

We used a series of experimental approaches to validate the bioinformatics analysis results and determined that overexpression of KIF3A suppressed, while KIF3A knockdown promoted the proliferation and migration of NPC cells, supporting the notion that KIF3A functions as a tumor suppressor in NPC. Previous studies have shown that KIF3A is oncogenic in prostate cancer, triple-negative breast cancer and bladder cancer but is tumor suppressive in lung cancer, which is consistent with our findings in NPC [17-19, 23].

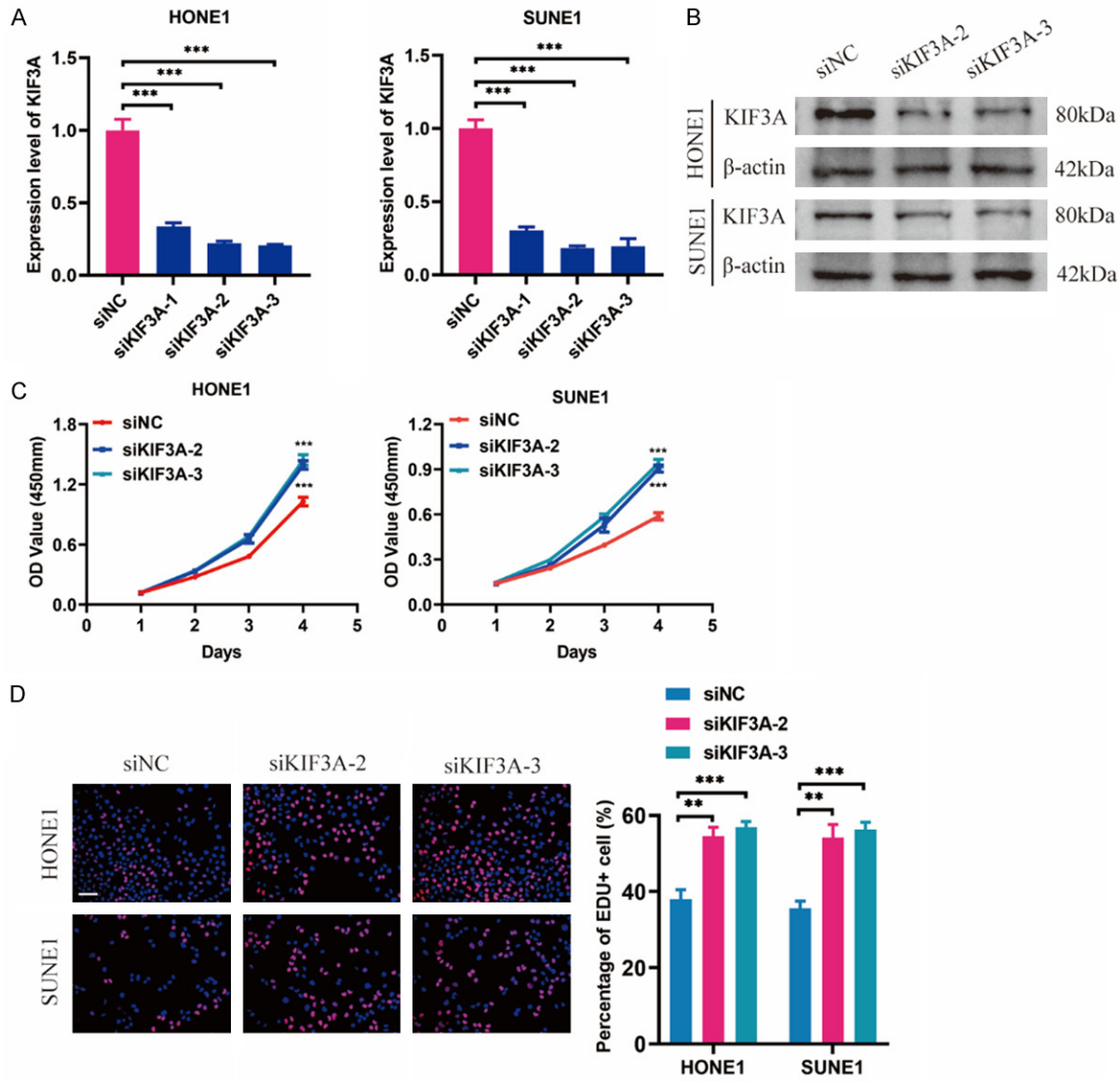

Figure 4. Knockdown of KIF3A promotes NPC cell proliferation. (A) qRT-PCR and (B) Western blot were conducted to evaluate KIF3A mRNA and protein level in the siNC, siKIF3A-2 and siKIF3A-3 groups. (C) CCK-8 and (D) EdU incorporation assays were performed after transfection with siNC/siKIF3A-2/siKIF3A-3 (Scale bar: 100 μm). Results were presented as the mean ± SD, Student's t test, **P < 0.01, ***P < 0.001.

EMT, a downstream event of Wnt/beta-catenin signaling, has been considered essential for tumor progression, invasion, metastasis [25, 26]. EMT involves the changes in cell adhesion and cytoskeleton re-organization [27-29]. In our study, we observed that the expression of the EMT-related proteins N-cadherin and Vimentin was downregulated by KIF3A overexpression and upregulated by KIF3A knockdown. However, in triple-negative breast cancer, knockdown of KIF3A expression reduced Vimentin protein expression and enhanced E-cadherin protein expression, which is contrary to our results [18]. Hence, the effect of KIF3A may be cancer type specific.

Cell cycle regulators are crucial for modulating tumor growth [30]. A previous study reported that KIF3A inhibition decreased the expression of CCND1, a downstream target of Wnt/β-catenin signaling in prostate cancer [17]. In addition, downregulated KIF3A expression also reduced CCND1 expression in triple-negative breast cancer [18]. However, KIF3A negatively modulated CCND1 expression in lung cancer [23]. In our study, we observed that overexpres-

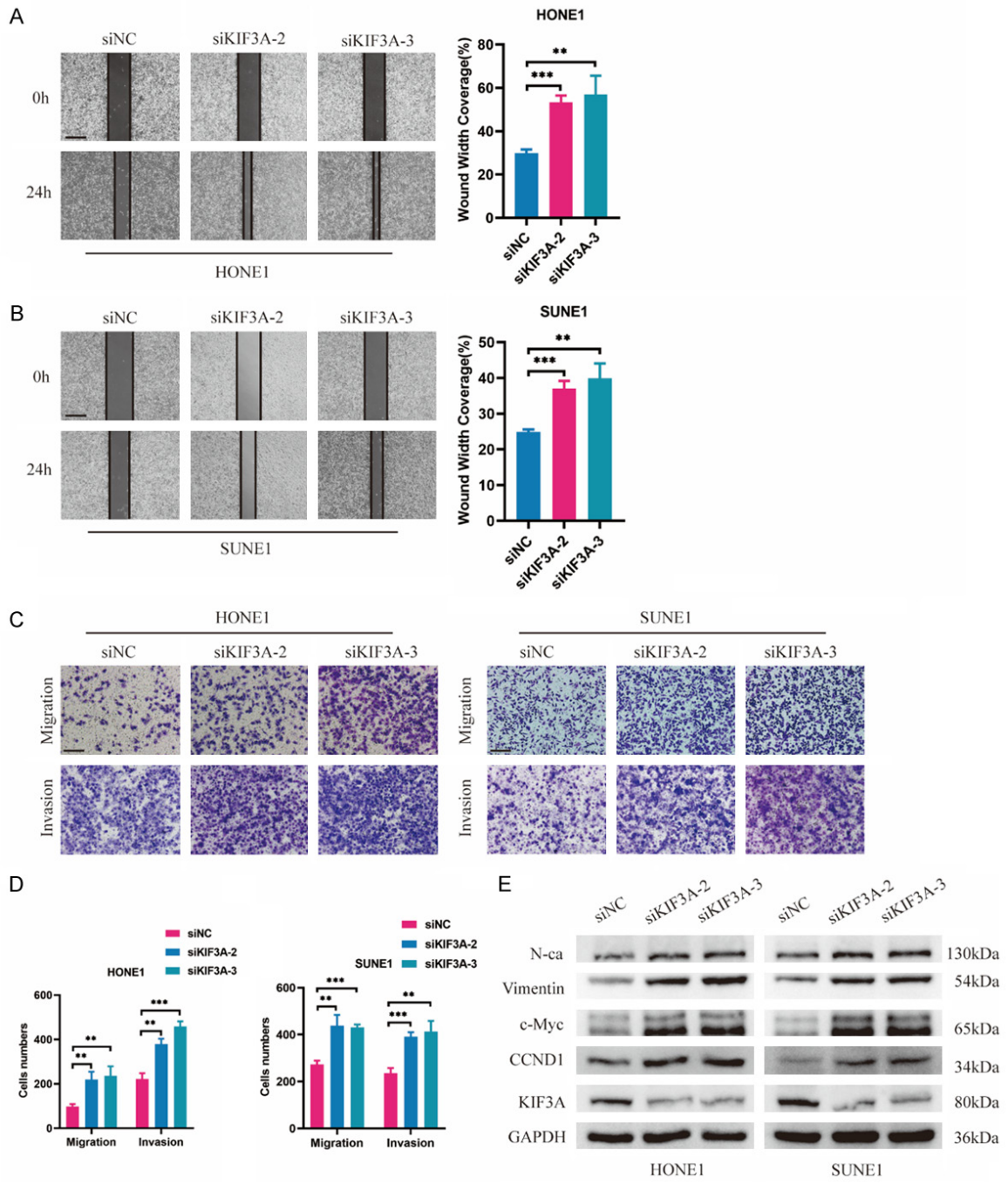

Figure 5. Knockdown of KIF3A promotes NPC cell migration and invasion. A, B. Wound healing assay showed that the migratory ability of HONE1 and SUNE1 cells was increased by KIF3A knockdown (Scale bar: 200 μm). C, D. Transwell assays indicated that the migratory ability of HONE1 and SUNE1 cells was increased by KIF3A knockdown (Scale bar: 200 μm). E. The expression levels of N-cadherin, Vimentin, c-Myc and CCND1 in HONE1 and SUNE1 cells were measured by western blot. Results were presented as the mean ± SD, Student's t test, **P < 0.01, ***P < 0.001.

sion of KIF3A inhibited CCND1 protein expression, consistent with the finding in lung cancer. Our study also found that c-Myc, an oncogene upstream of CCND1, was negatively modulated by KIF3A.

When exploring the potential KIF3A-interacting proteins using BioGRID database, β-catenin was suggested as a candidate. Encouraged by the report that KIF3A and β-catenin formed complex during spermatogenesis in *E. sinensis*

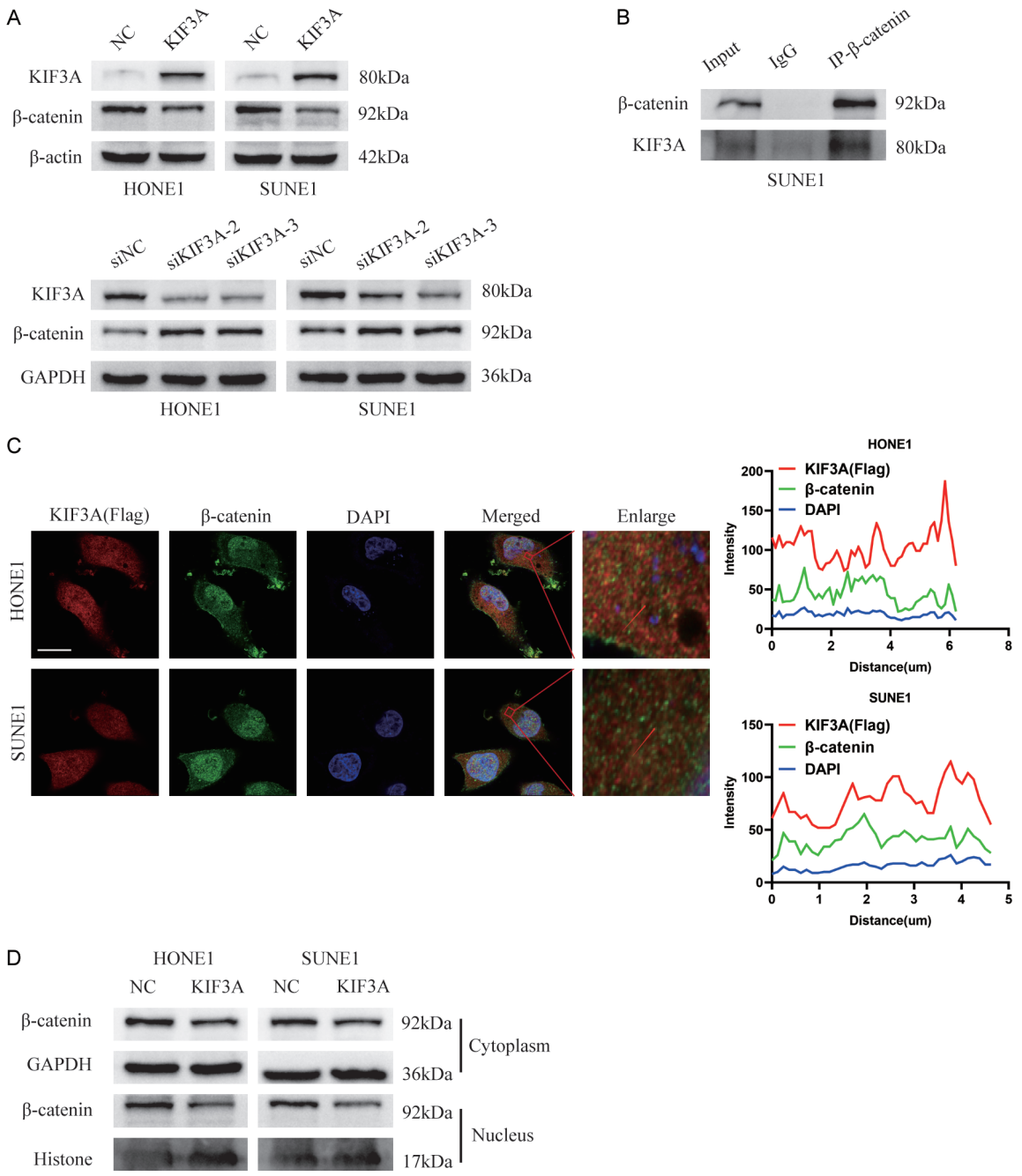

Figure 6. KIF3A interacts with β-catenin and suppresses its nuclear translocation. A. The expression levels of β-catenin in HONE1 and SUNE1 cells were measured by western blot. B. Co-IP assay was performed to detect the interaction between KIF3A and β-catenin in SUNE1 cell. C. Colocalization of KIF3A and β-catenin as determined by immunofluorescence in HONE1 and SUNE1 cells (Scale bar: 25 μm). D. The expression of β-catenin in the nucleus and cytoplasm was determined by western blot. GAPDH was used as the loading control of cytoplasm, while histone was used as the loading control of nucleus.

[31], we evaluated the interaction between KIF3A and β-catenin in NPC by co-IP experiments and found that KIF3A bound to β-catenin and inhibited β-catenin activation in NPC. Subsequent confocal microscopy demonstrated the colocalization of KIF3A and β-catenin in both cytosol and nucleus. β-catenin has been recognized as a critical regulator in the Wnt/β-catenin signaling pathway. Numerous studies have indicated that Wnt/β-catenin signaling regulates cell differentiation, proliferation, transcription, organogenesis, stemness, and can-

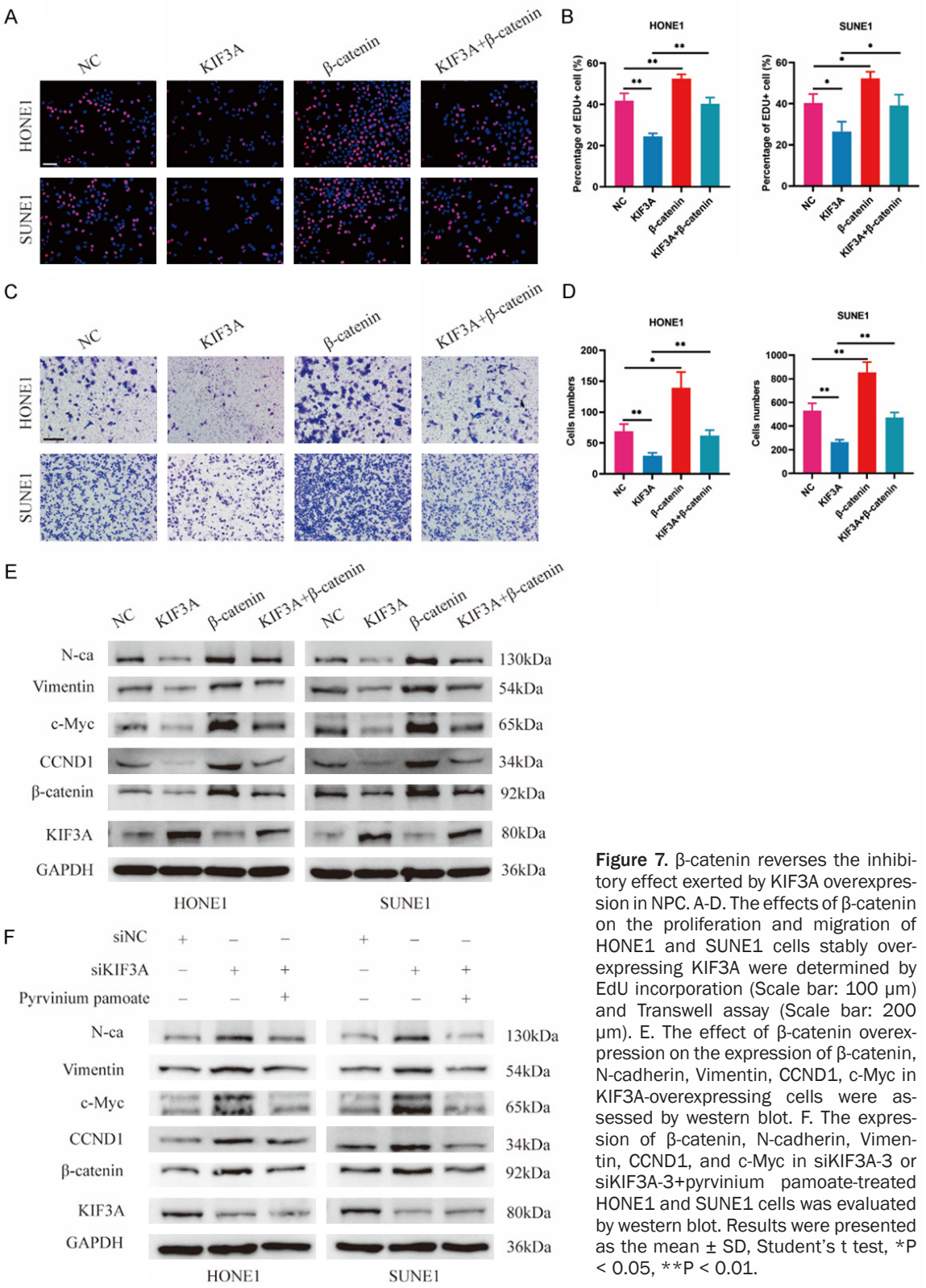

Figure 7. β-catenin reverses the inhibitory effect exerted by KIF3A overexpression in NPC. A-D. The effects of β-catenin on the proliferation and migration of HONE1 and SUNE1 cells stably overexpressing KIF3A were determined by EdU incorporation (Scale bar: 100 μm) and Transwell assay (Scale bar: 200 μm). E. The effect of β-catenin overexpression on the expression of β-catenin, N-cadherin, Vimentin, CCND1, c-Myc in KIF3A-overexpressing cells were assessed by western blot. F. The expression of β-catenin, N-cadherin, Vimentin, CCND1, and c-Myc in siKIF3A-3 or siKIF3A-3+pyrvinium pamoate-treated HONE1 and SUNE1 cells was evaluated by western blot. Results were presented as the mean ± SD, Student's t test, *P < 0.05, **P < 0.01.

cer metastasis [32-37]. In the Wnt/β-catenin pathway, the β-catenin degradation complex is composed of GKS3β, APC and Axin. This complex induces the phosphorylation of β-catenin, and phosphorylated β-catenin is subsequently labelled by ubiquitin for degradation by the pro-

teasome system [38], leading to decreased accumulation of β-catenin in the cytosol, which in turn inhibits its nuclear translocation.

In this study, we examined the effect of KIF3A overexpression on the nuclear/cytoplasmic distribution of β-catenin and observed a decreased β-catenin level in both cytoplasm and nucleus, suggesting that KIF3A overexpression reduced the accumulation of β-catenin in the cytosol, which in turn attenuated its nuclear translocation.

Nuclear accumulation of β-catenin is a hallmark of Wnt signaling activation [39]. An early study has shown that loss of KIF3A can induce CKI to promote Dvl phosphorylation and stabilize β-catenin in the cytosol, thereby leading to β-catenin accumulation in the nucleus and ultimately activating Wnt transcription [40]. In a previous mechanistic study, KIF3A was found to activate the Wnt/β-catenin pathway by enhancing the phosphorylation of DVL2 and the expression of cell cycle regulator CCND1 in prostate cancer. In addition, KIF3A was reported to modulate β-catenin/TCF-driven transcription [17]. A subsequent study in lung cancer indicated that KIF3A inhibited β-catenin level by interacting with β-arrestin to modulate the Wnt/β-catenin pathway, and knockdown of KIF3A activated β-catenin driven transcription, Moreover, high KIF3A expression was correlated with a reduction in CCND1 expression [23]. In our study, we also observed that KIF3A suppresses the malignancy of NPC by inhibiting the Wnt/β-catenin pathway. Taken together, these studies indicate the involvement of Wnt/β-catenin pathway in KIF3A-regulated tumor development.

In summary, this study demonstrated that KIF3A functions as a tumor suppressor and its decreased expression results in poor prognosis of NPC patients. Additionally, mechanistic analysis revealed that KIF3A interacts with β-catenin and inactivates the Wnt/β-catenin signaling pathway by attenuating β-catenin nuclear translocation, which in turn further inhibits its β-catenin-induced downstream cell cycle regulator expression and EMT signaling, thus attenuating NPC proliferation, migration, and invasion. Our study demonstrates the vital role of the KIF3A/β-catenin complex in NPC pathogenesis, which may serve as a potential therapeutic target for the treatment of patients with NPC.

Acknowledgements

We thank Springer Nature's English Language Editing service for editing the manuscript. This work was supported by the Project of Department of Education of Guangdong Provincial (2020KTSCX062).

Disclosure of conflict of interest

None.

Address correspondence to: Dr. Yan Xu, Cancer Center, Integrated Hospital of Traditional Chinese Medicine, Southern Medical University, The Compound at No. 13 Shiliugang Road, Haizhu District, Guangzhou 510315, Guangdong, China. E-mail: xuyan802000@163.com

References

[1] Tsao SW, Yip YL, Tsang CM, Pang PS, Lau VM, Zhang G and Lo KW. Etiological factors of nasopharyngeal carcinoma. Oral Oncol 2014; 50: 330-338.

[2] Li Y, Liu X, Lin X, Zhao M, Xiao Y, Liu C, Liang Z, Lin Z, Yi R, Tang Z, Liu J, Li X, Jiang Q, Li L, Xie Y, Liu Z and Fang W. Chemical compound cinobufotalin potently induces FOXO1-stimulated cisplatin sensitivity by antagonizing its binding partner MYH9. Signal Transduct Target Ther 2019; 4: 48.

[3] Chen YP, Chan ATC, Le QT, Blanchard P, Sun Y and Ma J. Nasopharyngeal carcinoma. Lancet (London, England) 2019; 394: 64-80.

[4] Tang Z, Chen W, Xu Y, Lin X, Liu X, Li Y, Liu Y, Luo Z, Liu Z, Fang W and Zhao M. MiR-4721, induced by EBV-miR-BART22, targets GSK3β to enhance the tumorigenic capacity of NPC through the WNT/β-catenin pathway. Mol Ther Nucleic Acids 2020; 22: 557-571.

[5] Liu Y, Jiang Q, Liu X, Lin X, Tang Z, Liu C, Zhou J, Zhao M, Li X, Cheng Z, Li L, Xie Y, Liu Z and Fang W. Cinobufotalin powerfully reversed EBV-miR-BART22-induced cisplatin resistance via stimulating MAP2K4 to antagonize nonmuscle myosin heavy chain IIA/glycogen synthase 3β/β-catenin signaling pathway. EBioMedicine 2019; 48: 386-404.

[6] Liang Z, Liu Z, Cheng C, Wang H, Deng X, Liu J, Liu C, Li Y and Fang W. VPS33B interacts with NESG1 to modulate EGFR/PI3K/AKT/c-Myc/P53/miR-133a-3p signaling and induce 5-fluorouracil sensitivity in nasopharyngeal carcinoma. Cell Death Dis 2019; 10: 305.

[7] Sung H, Ferlay J, Siegel RL, Laversanne M, Soerjomataram I, Jemal A and Bray F. Global cancer statistics 2020: GLOBOCAN estimates of incidence and mortality worldwide for 36 can-

cers in 185 countries. CA Cancer J Clin 2021; 71: 209-249.
[8] Engelke MF, Waas B, Kearns SE, Suber A, Boss A, Allen BL and Verhey KJ. Acute inhibition of heterotrimeric kinesin-2 function reveals mechanisms of intraflagellar transport in mammalian cilia. Curr Biol 2019; 29: 1137-1148, e4.
[9] Huangfu D, Liu A, Rakeman AS, Murcia NS, Niswander L and Anderson KV. Hedgehog signalling in the mouse requires intraflagellar transport proteins. Nature 2003; 426: 83-87.
[10] Hirokawa N and Noda Y. Intracellular transport and kinesin superfamily proteins, KIFs: structure, function, and dynamics. Physiol Rev 2008; 88: 1089-1118.
[11] Hirokawa N and Takemura R. Molecular motors and mechanisms of directional transport in neurons. Nat Rev Neurosci 2005; 6: 201-214.
[12] Cullen CL, O'Rourke M, Beasley SJ, Auderset L, Zhen Y, Pepper RE, Gasperini R and Young KM. Kif3a deletion prevents primary cilia assembly on oligodendrocyte progenitor cells, reduces oligodendrogenesis and impairs fine motor function. Glia 2021; 69: 1184-1203.
[13] Huang CJ, Huang CC and Chang CC. Association of the testis-specific TRIM/RBCC protein RNF33/TRIM60 with the cytoplasmic motor proteins KIF3A and KIF3B. Mol Cell Biochem 2012; 360: 121-131.
[14] Deeb SK, Guzik-Lendrum S, Jeffrey JD and Gilbert SP. The ability of the kinesin-2 heterodimer KIF3AC to navigate microtubule networks is provided by the KIF3A motor domain. J Biol Chem 2019; 294: 20070-20083.
[15] Gaudin R, de Alencar BC, Jouve M, Bèrre S, Le Bouder E, Schindler M, Varthaman A, Gobert FX and Benaroch P. Critical role for the kinesin KIF3A in the HIV life cycle in primary human macrophages. J Cell Biol 2012; 199: 467-479.
[16] Xiong R, Rao P, Kim S, Li M, Wen X and Yuan W. Herpes simplex virus 1 US3 phosphorylates cellular KIF3A to downregulate CD1d expression. J Virol 2015; 89: 6646-6655.
[17] Liu Z, Rebowe RE, Wang Z, Li Y, Wang Z, DePaolo JS, Guo J, Qian C and Liu W. KIF3a promotes proliferation and invasion via Wnt signaling in advanced prostate cancer. Mol Cancer Res 2014; 12: 491-503.
[18] Wang W, Zhang R, Wang X, Wang N, Zhao J, Wei Z, Xiang F and Wang C. Suppression of KIF3A inhibits triple negative breast cancer growth and metastasis by repressing Rb-E2F signaling and epithelial-mesenchymal transition. Cancer Sci 2020; 111: 1422-1434.
[19] Zhou Q, Yu J, Zheng Q, Wu T, Ji Z and Zhuo Y. Kinesin family member 3A stimulates cell proliferation, migration, and invasion of bladder cancer cells in vitro and in vivo. FEBS Open Bio 2021; 11: 1487-1496.
[20] Barakat MT, Humke EW and Scott MP. Kif3a is necessary for initiation and maintenance of medulloblastoma. Carcinogenesis 2013; 34: 1382-1392.
[21] Lehmann H, Vicari D, Wild PJ and Frew IJ. Combined deletion of Vhl and Kif3a accelerates renal cyst formation. J Am Soc Nephrol 2015; 26: 2778-2788.
[22] Lee J, Park KC, Sul HJ, Hong HJ, Kim KH, Kero J and Shong M. Loss of primary cilia promotes mitochondria-dependent apoptosis in thyroid cancer. Sci Rep 2021; 11: 4181.
[23] Kim M, Suh YA, Oh JH, Lee BR, Kim J and Jang SJ. KIF3A binds to β-arrestin for suppressing Wnt/β-catenin signalling independently of primary cilia in lung cancer. Sci Rep 2016; 6: 32770.
[24] Yang Y, Liu X, Li R, Zhang M, Wang H and Qu Y. Kinesin family member 3A inhibits the carcinogenesis of non-small cell lung cancer and prolongs survival. Oncol Lett 2020; 20: 348.
[25] Ding W, You H, Dang H, LeBlanc F, Galicia V, Lu SC, Stiles B and Rountree CB. Epithelial-to-mesenchymal transition of murine liver tumor cells promotes invasion. Hepatology (Baltimore, Md.) 2010; 52: 945-953.
[26] Pastushenko I and Blanpain C. EMT transition states during tumor progression and metastasis. Trends Cell Biol 2019; 29: 212-226.
[27] Derynck R and Weinberg RA. EMT and cancer: more than meets the eye. Dev Cell 2019; 49: 313-316.
[28] Zhou P, Li B, Liu F, Zhang M, Wang Q, Liu Y, Yao Y and Li D. The epithelial to mesenchymal transition (EMT) and cancer stem cells: implication for treatment resistance in pancreatic cancer. Mol Cancer 2017; 16: 52.
[29] Lamouille S, Xu J and Derynck R. Molecular mechanisms of epithelial-mesenchymal transition. Nat Rev Mol Cell Biol 2014; 15: 178-196.
[30] Qie S and Diehl JA. Cyclin D1, cancer progression, and opportunities in cancer treatment. J Mol Med (Berl) 2016; 94: 1313-1326.
[31] Liang YJ, Ni JH, Wang LM, Tan FQ and Yang WX. KIF3A regulates the Wnt/β-catenin pathway via transporting β-catenin during spermatogenesis in Eriocheir sinensis. Cell Tissue Res 2020; 381: 527-541.
[32] Krishnamurthy N and Kurzrock R. Targeting the Wnt/beta-catenin pathway in cancer: update on effectors and inhibitors. Cancer Treat Rev 2018; 62: 50-60.
[33] Zhan T, Rindtorff N and Boutros M. Wnt signaling in cancer. Oncogene 2017; 36: 1461-1473.
[34] Luke JJ, Bao R, Sweis RF, Spranger S and Gajewski TF. WNT/β-catenin pathway activation correlates with immune exclusion across hu-

man cancers. Clin Cancer Res 2019; 25: 3074-3083.
[35] Clevers H and Nusse R. Wnt/β-catenin signaling and disease. Cell 2012; 149: 1192-1205.
[36] Fodde R and Brabletz T. Wnt/beta-catenin signaling in cancer stemness and malignant behavior. Curr Opin Cell Biol 2007; 19: 150-158.
[37] Rosenbluh J, Nijhawan D, Cox AG, Li X, Neal JT, Schafer EJ, Zack TI, Wang X, Tsherniak A, Schinzel AC, Shao DD, Schumacher SE, Weir BA, Vazquez F, Cowley GS, Root DE, Mesirov JP, Beroukhim R, Kuo CJ, Goessling W and Hahn WC. β-Catenin-driven cancers require a YAP1 transcriptional complex for survival and tumorigenesis. Cell 2012; 151: 1457-1473.
[38] Stamos JL and Weis WI. The β-catenin destruction complex. Cold Spring Harb Perspect Biol 2013; 5: a007898.
[39] Nusse R. Wnt signaling in disease and in development. Cell Res 2005; 15: 28-32.
[40] Corbit KC, Shyer AE, Dowdle WE, Gaulden J, Singla V, Chen MH, Chuang PT and Reiter JF. Kif3a constrains β-catenin-dependent Wnt signalling through dual ciliary and non-ciliary mechanisms. Nat Cell Biol 2008; 10: 70-76.